Histamine Deficiency Decreases Atherosclerosis and Inflammatory Response in Apolipoprotein E Knockout Mice Independently of Serum Cholesterol Level

Ke-Yong Wang, Akihide Tanimoto, Xin Guo, Sohsuke Yamada, Shohei Shimajiri, Yoshitaka Murata, Yan Ding, Masato Tsutsui, Seiya Kato, Teruo Watanabe, Hiroshi Ohtsu, Ken-Ichi Hirano, Kimitoshi Kohno, Yasuyuki Sasaguri

Objective—Histamine and histamine receptors are found in atherosclerotic lesions, and their signaling and subsequent proatherogenic or proinflammatory gene expression are involved in atherogenesis. In the present study, we generated apolipoprotein E (apoE) and histamine synthesizing histidine decarboxylase double knockout (DKO) mice on a C57BL/6J (wild-type mice) background to clarify the roles of histamine in atherosclerosis.

Methods and Results—Wild-type, apoE knockout (KO), and DKO mice were fed a high-cholesterol diet to analyze hyperlipidemia-induced atherosclerosis. Compared with wild-type mice, apoE-KO mice showed increased expression of histamine and its receptors, corresponding to increased atherosclerotic lesion areas and expression of inflammatory regulators, such as nuclear factor-κB, scavenger receptors, inflammatory cytokines, and matrix metalloproteinases. Histamine deficiency after deletion of histidine decarboxylase reduced atherosclerotic areas and expression of a range of the inflammation regulatory genes, but serum cholesterol levels of DKO mice were higher than those of apoE-KO mice.

Conclusion—These results indicate that histamine is involved in the development of atherosclerosis in apoE-KO mice by regulating gene expression of inflammatory modulators, an action that appears to be independent of serum cholesterol levels. In addition to acute inflammatory response, histamine participates in chronic inflammation, such as hyperlipidemia-induced atherosclerosis, and might be a novel therapeutic target for the treatment of atherosclerosis. (***Arterioscler Thromb Vasc Biol.* 2011;31:00-00.)**

Key Words: histamine ■ histidine decarboxylase ■ hyperlipidemia-induced atherosclerosis ■ inflammation ■ matrix metalloproteinase

Recently, evidence has emerged concerning inflammatory mechanisms of the initiation and progression of atherosclerosis.[1,2] Histamine, one of the classical inflammatory mediators, is synthesized from L-histidine by a rate-limiting enzyme, histidine decarboxylase (HDC). Histamine is released from mast cells and mediates type I hypersensitivity via histamine receptor H1 (HH1R),[3] and histamine produced by enterochromaffin-like cells induces gastric acid secretion from parietal cells via histamine receptor H2 (HH2R).[4] In the field of cardiovascular pathology, accumulation of activated mast cells and histamine in the coronary adventitia has been implicated in progression of plaque rupture and acute coronary syndrome.[5–7] In addition, several epidemiological studies have reported an enhancement of atherosclerosis in the patients of allergy or increased blood histamine.[8–10] Together, these suggest a possible involvement of histamine in the pathogenesis of atherosclerosis and related disorders.

Previously, we demonstrated that HDC-knockout (KO) mice showed reduced neointimal formation induced by ligation of the carotid artery or cuff replacement of the femoral artery.[11] Because histamine stimulates smooth muscle cells (SMCs) to proliferate and SMCs predominantly express HH1R,[12] the neointimal formation, which consists of SMCs, is suggested to be an HH1R-mediated response.[11] Although ligation- or cuff-induced intimal hyperplasia mimics diffuse intimal thickening as a precursor lesion of atherosclerosis,[13] it is quite different from established atherosclerosis, in which accumulation of lipid-laden macrophages has a unique his-

Received on: August 26, 2010; final version accepted on: January 13, 2011.

From the Departments of Pathology and Cell Biology (K.-Y.W., A.T., X.G., S.Y., S.S., Y.D., Y.S.) and Molecular Biology (K.K.), School of Medicine, University of Occupational and Environmental Health, Kitakyushu, Japan; Department of Molecular and Cellular Pathology, Kagoshima University Graduate School of Medical and Dental Sciences, Kagoshima, Japan (A.T.); Kyurin Omtest Laboratory Department, Kyurin Corp, Kitakyushu, Japan (Y.M.); Departments of Pharmacology (M.T.) and Pathology and Cell Biology (S.K.), Graduate School and Faculty of Medicine, University of the Ryukyus, Okinawa, Japan; Laboratory of Pathology, Fukuoka Wajiro Hospital, Fukuoka, Japan (T.W.); Department of Applied Quantum Medical Engineering, Tohoku University, Sendai, Japan (H.O.); Department of Cardiovascular Medicine, Graduate School of Medicine, Osaka University, Osaka, Japan (K.-I.H.).

Correspondence to Yasuyuki Sasaguri, MD, PhD, Department of Pathology and Cell Biology, School of Medicine, University of Occupational and Environmental Health, 1-1 Iseigaoka, Yahatanishi-ku, Kitakyushu 807-8555, Japan. E-mail yasu3219@med.uoeh-u.ac.jp

Arterioscler Thromb Vasc Biol **is available at http://atvb.ahajournals.org** **DOI: 10.1161/ATVBAHA.110.215228**

Table 1. Primers Used for Real-Time PCR

Gene*	Forward Primer	Reverse Primer	TaqMan Probe
CD106 (VCAM-1)	CTCATTCCCTGAAGATCCAGTAATTAA	TCAAAGGGATACACATTAGGGACTGT	TGAGTGGGCCACTTGTGCATGGG
CD36	AGGTCCTTACACATACAGAGTTCGTTATC	AACAGACAGTGAAGGCTCAAAGATG	ACTCAGGACCCCGAGGACCACACTG
CD54 (ICAM-1)	CAAACAGGAGATGAATGGTACATACG	ACCAGAATGATTATAGTCCAGTTATTTTGAG	CCATGGGAATGTCACCAGGAATGTGTACC
HDC	CAAATGTGCAGCCTGGATACC	CGTTCAATGTCCCCAAAGATG	AGTGCTCCCGAGGAACCCGACAG
HH1R	CTTTAGTGTCTTCATCCTGTGTATTGATC	GTAGCTGAAGCACGGGTCTTG	TGTCCAGCAACCCCTCCGGTACCT
HH2R	CCTTCTCTGCCATTTACCAGTTG	CATCACATCCAGGCTGGTGTAG	AGTGGAGGTTTGGCCAGGTCTTCTGC
IL1-β	TGCACTACAGGCTCCGAGATG	GTACAAAGCTCATGGAGAATATCACTTG	TGTCGGACCCATATGAGCTGAAAGCTCTC
IL1R1	AGTTAAAAGCCAGTTTTATCGCTATCC	CCCCCGATGAGGTAATTCTTG	AAATATTTTTGAGTCGGCGCATGTGCAGTTAAT
IL6	TTACACATGTTCTCTGGGAAATCG	TTGGTAGCATCCATCATTTCTTTG	TGAGAAAAGAGTTGTGCAATGGCAATTCTGAT
iNOS	GCAGTGGAGAGATTTTGCATGAC	ATGGACCCCAAGCAAGACTTG	CACCACAAGGCCACATCGGATTTCAC
LDLR	CCAAATGGCATCACACTAGATCTTT	GGTTCTCATCCTCCAAAATGGTT	TTGGGTTGATTCCAAACTCCACTCTATCTCCA
LOX-1	GTCATCCTCTGCCTGGTGTTG	AGTAAGGTTCGCTTGGTATTGTTTTAAG	TATTGTACAGTGGACACAATTACGCCA
MCP-1	GGCTCAGCCAGATGCAGTTAAC	GCCTACTCATTGGGATCATCTTG	CCCACTCACCTGCTGCTACTCATTCACC
MMP-2	CTTCACTTTCCTGGGCAACAAG	CTGCCACGAGGAATAGGCTATATC	AACCAACTACGATGATGACCGGAAGTG
MMP-3	GAGGAAATCCCACATCACCTACAG	ACCTCCTCCCAGACCTTCAAAG	ACCGGATTTGCCAAGACAGAGTGTGGAT
MMP-9	TTGAGTCCGGCAGACAATCC	CCCTGTAATGGGCTTCCTCTATG	TGATGCTATTGCTGAGATCCAGGGCG
MMP-12	GTGCCCGATGTACAGCATCTTAG	AGTCTACATCCTCACGCTTCATGTC	CGGTACCTCACTTACAGGATCTATAATTACA
PDGF-β	ACCTCGCCTGCAAGTGTGA	CTCGCTGCTCCCTGGATGT	AGTGACCCCTCGGCCTGTGACTAGAAGTC
SR-A	ACACTGCTTGATGTTCAACTCCATAC	TTTGTACACACGTTCCTCCAATTTAC	TGTCAGAGTCCGTGAATCTACAGCAAAGCAAC
SR-BI	TGGGACTTCCGGGCAGAT	GCCTCCGGGCTGAAGAAT	ACCCTTCATGACACCCGAATCCTCG
TNFR2	TGGTCTGATTGTTGGAGTGACATC	GGATTTCTCATCAGGCACATGAG	TGCATCATCCTGGTGCAGAGGAAAAAGA
18s rRNA	TaqMan Ribosomal RNA Control Reagents VIC Probe (Applied Biosystems, catalog no. 4308329)		

*iNOS indicates inducible nitric oxide synthase; PDGF, platelet-derived growth factor; TNFR, tumor necrosis factor receptor.

tology. Interestingly, infiltrating macrophages in the atherosclerotic lesions express HDC as a source of histamine in human carotid arteries and the aortas of apolipoprotein E (apoE)–KO mice.[11,14,15] HDC expression in human monocytes is upregulated during macrophage differentiation, which corresponds to a switch of the histamine receptor profile from HH2R predominance in monocytes to HH1R dominance in macrophages.[16,17] Together, these results indicate that both histamine production and response is present in the cells, constituting atherosclerotic lesions and that macrophage-derived histamine could regulate atherogenic response.[18] However, the roles of histamine in the process of hyperlipidemia-induced atherosclerosis still remain unclear.

To further the examination, we generated HDC and apoE double-knockout (DKO) mice to investigate the roles of histamine in hyperlipidemia-induced atherosclerosis. The expression of inflammatory cytokines, scavenger receptors (SRs), matrix metalloproteinases (MMPs), and nuclear factor-κB (NF-κB), which regulate inflammatory response in the atherosclerotic lesions, was studied by reverse transcription–polymerase chain reaction (RT-PCR), Western blotting, and immunohistochemistry. In addition, we studied the effects of histamine on serum cholesterol.

Materials and Methods

Animals

We generated DKO mice by crossing apoE-KO mice (Jackson Laboratory, Bar Harbor, ME) with previously generated HDC-KO mice.[19] Male mice were weaned at 8 weeks of age onto a high-cholesterol diet (HcD) consisting of 1.25% cholesterol, 15% lard, and 0.5% sodium cholate (Oriental Yeast Co, Tokyo, Japan) and were maintained on this diet for 12 weeks. Another group was maintained to 23 weeks and 33 weeks of age on a normal chow diet (NcD). Wild-type (WT) C57BL/6J mice (Charles River, Yokohama, Japan) were used for control groups. Each experimental group included at least 10 mice. Animals were maintained on a 12-hour light/dark cycle. All protocols were approved by the Ethics Committee of Animal Care and Experimentation, University of Occupational and Environmental Health, and were performed according to the institutional guidelines for animal experiments and according to Law 105 and Notification 6 of the Japanese government.

Assessment of Atherosclerosis and Immunohistochemistry

The aortas were cut open longitudinally and fixed with 10% neutral buffered formalin for 24 hours. Then the aortas were stained with Oil Red O stain. *En face* images of the aortas were captured with a digital camera. Oil Red O–stained area relative to whole surface area was calculated using NIH Image software. For histological analysis, formalin-fixed and paraffin-embedded tissues were sectioned, and every 10-step sections of 1-cm length ascending aortas from the aortic valve (4-μm-thick step sections: 1500 sections/aorta) were stained with hematoxylin and eosin stain. After scanning using a virtual slide system (NanoZoomer Digital Pathology, Hamamatsu Photonics, Hamamatsu, Japan), the intima/media ratio and intimal plaque area were evaluated using NIH Image.[11,20] Immunostaining was carried out (Envision kit, Dako) on the paraffin sections using antibodies against smooth muscle actin (clone 1A4, ×100, Dako), macrophages (Mac-3 clone M3/84, ×50, BD Bioscience Pharmingen, Tokyo, Japan), HDC (rabbit polyclonal, ×100; Progen Biotechnik, Heidelberg, Germany), and histamine (rabbit polyclonal, ×100; Progen Biotechnik) as previously described.[15] Immunolocalization of NF-κB was also studies in the atherosclerotic lesions (rabbit polyclonal, ×2000, Abcam).

Lipoprotein Analysis

After mice were starved for 7 hours, blood was collected, and the serum was analyzed by high-performance liquid chromatography (Skylight Biotech, Akita, Japan).[21]

Real-Time Polymerase Chain Reaction

Expression of mRNA in the liver and aortas was quantified by real-time RT-PCR using TaqMan quantitative PCR analysis. The genes investigated and primers for PCR are listed in Table 1.

Table 2. HPLC Analysis of Serum Lipoproteins

	Diet	Week	WT	ApoE-KO	DKO
T-cho (mg/dL)	NcD	23	68.3±2.7	325.0±35.4*	428.2±24.8*†
	NcD	33	78.3±3.7	365.5±52.0*	496.1±37.0*†
	HcD	12	166.5±8.4	470.1±61.1*	633.5±50.8*†
VLDL (mg/dL)	NcD	23	3.9±0.6	137.7±22.8*	225.7±14.1*†
	NcD	33	6.1±0.8	208.5±34.4*	283.4±24.4*†
	HcD	12	63.7±6.1	284.8±39.1*	381.4±30.9*†
LDL (mg/dL)	NcD	23	7.5±0.3	94.5±10.3*	153.6±10.5*†
	NcD	33	9.0±0.6	107.5±17.6*	161.7±10.5*†
	HcD	12	39.2±2.6	108.4±19.9*	165.3±10.7*†
HDL (mg/dL)	NcD	23	56.9±2.0	26.2±2.8*	36.6±3.6*†
	NcD	33	63.7±2.8	28.3±1.4*	35.6±2.2*†
	HcD	12	60.9±3.1	23.0±2.1*	32.5±4.2*†

VLDL indicates very-low-density lipoprotein.
*$P<0.05$ vs WT.
†$P<0.05$ vs apoE-KO.

Measurement of Histamine and Monocyte Chemoattractant Protein-1 in Serum and Aortic Tissue

The aortic and serum levels of monocyte chemoattractant protein-1 (MCP-1) and histamine were measured by ELISA (R&D Systems and Immunotech, Marseille, France). The aortas were homogenized in 0.2 N $HClO_4$ buffer (100 μL/10 μg tissue), and the supernatants were collected by centrifugation (10,000*g* for 5 minutes at 4°C). After neutralization by addition of an equal volume of 1 mol/L potassium borate (pH 9.25) and measurement of protein concentration, the supernatants were subjected to ELISA.

Western Blotting

The aortic expression of class A SR (SR-A), CD36 (rabbit polyclonal, ×1000; Santa Cruz Biotechnology), and NF-κB (rabbit polyclonal, ×2000, Abcam) proteins was studied by Western blotting.

Statistical Analysis

ANOVA was applied to determine statistical differences, and a probability value of less than 0.05 was taken to be significant.

Results

General Phenotypes of DKO Mice

The body weight of apoE-KO mice was not increased, and that of WT and DKO mice was increased after NcD for 33 weeks (Supplemental Figure IA, available online at http://atvb.ahajournals.org). Both systolic and diastolic blood pressure was increased in apoE-KO mice compared with WT mice. In DKO mice, blood pressure was decreased to the level of WT mice (Supplemental Figure IB). White blood cell counts were not different among WT, apoE-KO, and DKO mice, but percentages of neutrophiles and lymphocytes were increased in apoE-KO mice. Very few basophiles were observed in the peripheral blood from WT, apoE-KO, and DKO mice (Supplemental Table I). No infectious diseases or other pathological conditions were observed during the experiments in the mice.

Serum Cholesterol Levels in DKO Mice

On feeding with NcD for 23 to 33 weeks or with HcD for 12 weeks from the age of 8 weeks, apoE-KO and DKO mice became hyperlipidemic, with increased total cholesterol, very-low-density lipoprotein cholesterol, and low-density lipoprotein (LDL) cholesterol but decreased high-density lipoprotein (HDL) cholesterol compared with WT mice (Table 2). Furthermore, compared with apoE-KO mice, DKO mice showed higher cholesterol levels in all fractions, but HDL cholesterol was moderately increased in DKO mice.

Induction of Histamine and Histamine Receptors by Hyperlipidemia

Serum histamine levels were increased in apoE-KO mice compared with WT mice during the ages of 23 to 33 weeks with NcD (Figure 1A). After 12 weeks of feeding with HcD, serum histamine levels were markedly higher than values for feeding with NcD (Figure 1B). In DKO mice, serum histamine was not detected (Figure 1A and 1B). Real-time RT-PCR showed increased HDC expression in atherosclerotic aortas of apoE-KO

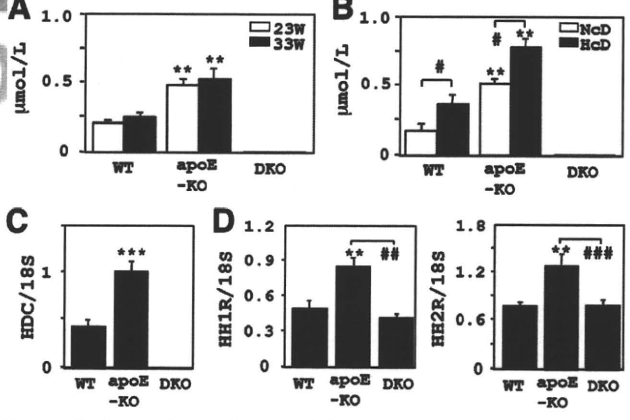

Figure 1. Serum histamine and HDC, HH1R, and HH2R expression in aortic tissue. A and B, Serum histamine was increased in apoE-KO mice but not in histamine-deficient DKO mice. From 23 to 33 weeks of age with NcD, serum histamine increased in apoE-KO mice (A), and HcD feeding for 12 weeks much increased serum histamine levels (B). C and D, Aortic expression of HDC, HH1R, and HH2R was increased in apoE-KO mice fed HcD for 12 weeks. The expression of HH1R and HH2R in DKO mice was decreased compared with apoE-KO mice. The values are presented as mean±SE. *$P<0.05$, **$P<0.01$, ***$P<0.001$ vs WT mice; ##$P<0.05$, ###$P<0.001$.

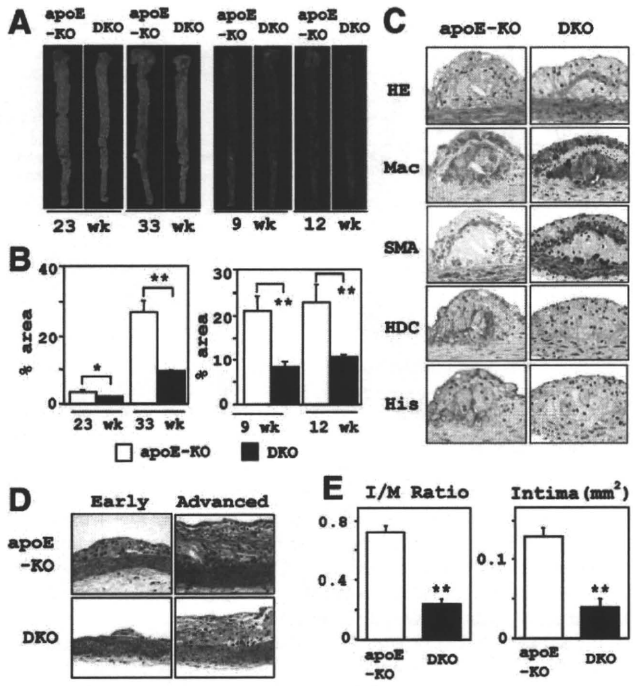

Figure 2. Quantitative analysis of hyperlipidemia-induced atherosclerosis. A, Oil Red O–stained atherosclerotic lesions in NcD-fed (for 23 and 33 weeks) and HcD-fed (9 and 12 weeks) mice. B, The atherosclerotic areas stained with Oil Red O stain were decreased in DKO mice fed NcD and HcD. The values are presented as mean±SE. $^{*}P<0.05$, $^{**}P<0.01$ vs apoE-KO mice. C and D, Representative microphotographs of the aortic lesions. E, Intima to media ratio (I/M ratio) in NcD-fed mice (33 weeks) evaluated from serial sections of the aorta. The values are presented as mean±SE. $^{**}P<0.01$ vs apoE-KO mice. HE indicates hematoxylin and eosin; Mac, macrophage; SMA, smooth muscle actin; His, histamine.

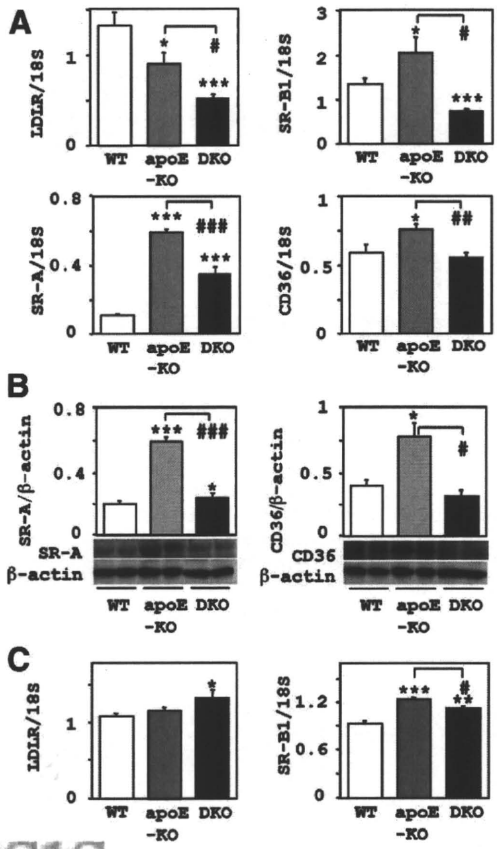

Figure 3. Expression of LDLR, SR-BI, and SRs in atherosclerotic aortas. A, Expression of LDLR and SRs in the aortas was analyzed in WT and KO mice fed HcD for 12 weeks. The expression of these genes was downregulated in DKO mice compared with apoE-KO mice. B, SR-A and CD36 expression in protein levels was studied by Western blotting. The expression levels in protein were correlated with those in mRNA. C, In the liver, SR-BI expression was decreased in DKO mice, but that of LDLR was increased in DKO mice compared with apoE-KO mice. Values were normalized by 18S rRNA expression (RT-PCR) or β-actin (Western blotting) expression and are presented as mean±SE. $^{*}P<0.05$, $^{**}P<0.01$, $^{***}P<0.001$ vs WT mice; $\#P<0.05$, $\#\#P<0.01$, $\#\#\#P<0.001$ vs apoE-KO mice.

mice fed HcD (Figure 1C). Expression of *HH1R*, *HH2R*, and *HH3R* but not *HH4R* in atherosclerotic aortas was increased in apoE-KO mice compared with WT mice after HcD feeding, whereas it was significantly decreased in DKO mice (Figure 1D and Supplemental Figure II).

Suppression of Hyperlipidemia-Induced Atherosclerosis in DKO Mice

En face analysis demonstrated that atherosclerotic lesion area was markedly increased during the age of 23 to 33 weeks in apoE-KO mice fed NcD, whereas it was much less in DKO mice (40% of apoE-KO mice) (Figure 2A). After mice were fed HcD for 9 or 12 weeks, atherosclerotic lesion area in DKO mice was also 40% of that of apoE-KO mice (Figure 2B). The atherosclerotic lesions of apoE-KO mice included Mac-3-positive macrophages (foam cells) and a lesser number of α-smooth muscle actin–positive SMCs. The macrophages were positive for HDC and histamine in apoE-KO mice (Figure 2C). In addition to the Mac-3-positive macrophages, a few CD3-positive T lymphocytes infiltrated in the atherosclerotic intima (data not shown). The T cell counts were increased in apoE-KO and DKO mice compared with WT mice, but they were not different between apoE-KO and DKO mice (Supplemental Table II).

Because mast cells in HDC-KO mice are decreased in number and show abnormal morphology and reduced granular content,[19] the mast cells in the atherosclerotic aortas were studied by toluidine blue stain. Mast cells were not observed in the atherosclerotic intima, but a few cells were detected in the adventitia, and no significant differences in these cell numbers were noted among WT, apoE-KO, and DKO mice (data not shown).

In 33-week-old mice fed NcD, intima/media ratio and intimal lesion area were significantly reduced by 60% in DKO mice compared with apoE-KO mice (Figure 2D and 2E). Mice fed HcD for 9 to 12 weeks had similar results (data not shown).

Expression of SRs and LDL Receptor in the Liver and Aortas in DKO Mice

Real-time RT-PCR revealed that expression of LDL receptor (LDLR) was decreased in both apoE-KO and DKO compared with WT mice but was further decreased in DKO mice compared with apoE-KO mice. SRs, including SR-A,[22] SR-BI,[23] CD36,[24] and lectin-like oxidized LDLR-1 (LOX-1)[25] were increased in apoE-KO mice fed HcD for 12 weeks. The expression of these SRs genes was significantly downregulated in DKO mice compared with apoE-KO mice (Figure 3A

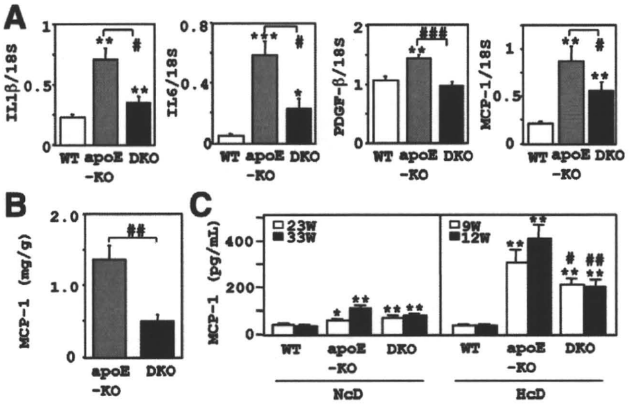

Figure 4. Expression of inflammatory factors in atherosclerotic aortas. A, Expression of inflammatory factors in the aorta was analyzed in WT, apoE-KO, and DKO mice fed HcD for 12 weeks. These genes expression were increased in apoE-KO mice but decreased in DKO mice. B, Aortic MCP-1 content in DKO mice was lower than that in apoE-KO mice in 12 weeks of HcD. C, Serum MCP-1 was increased in apoE-KO and DKO mice fed NcD from 23 to 33 weeks of age. After HcD feeding for 9 and 12 weeks, serum MCP-1 of both apoE-KO and DKO mice were increased compared with that of WT mice. Tissue MCP-1 was normalized by tissue weight. The mRNA expression was normalized by 18S rRNA expression and is presented as mean±SE. *$P<0.05$, **$P<0.01$, ***$P<0.001$ vs WT; #$P<0.05$, ##$P<0.01$ vs apoE-KO mice.

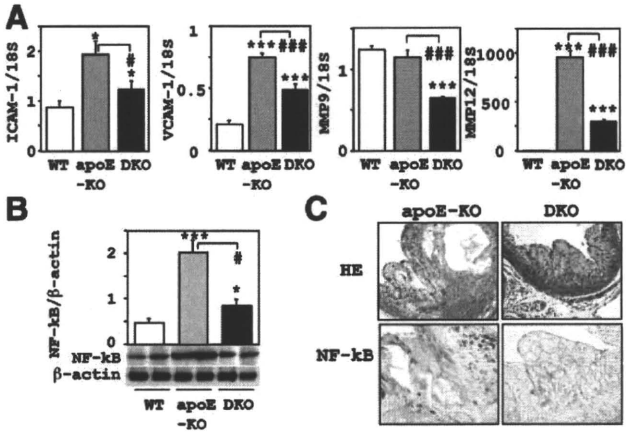

Figure 5. Expression of adhesion molecules, MMPs, and NF-κB. Expression of ICAM-1, VCAM-1, and MMPs in the aorta in WT, apoE-KO, and DKO mice fed HcD for 12 weeks. Values were normalized by 18S rRNA expression and are presented as mean±SE. A, ICAM-1 and VCAM-1 expression was increased in atherosclerotic aortas in apoE-KO mice and decreased in DKO mice. MMP expression was also increased in atherosclerotic plaques of apoE-KO mice, except for MMP-9, and was decreased in DKO mice. The expression of NF-κB was studied by Western blotting (B) and immunohistochemistry (C). In apoE-KO mice, NF-κB expression was increased and localized in the nuclei of the macrophages. Both expression and nuclear localization were decreased in DKO mice. *$P<0.05$, **$P<0.01$, ***$P<0.001$ vs WT mice; #$P<0.05$, ##$P<0.01$ vs apoE-KO mice.

and Supplemental Figure III). The levels of protein expression of SR-A and CD36 were correlated to those of mRNA expression (Figure 3B). In the liver, mRNA expression of *SR-BI* was moderately decreased in DKO mice, but that of *LDLR* was increased in DKO mice compared with apoE-KO mice (Figure 3C).

Suppression of Inflammatory Response in Atherosclerotic Aortas of DKO Mice

Expression of inflammatory cytokines or growth factors and their receptors, such as tumor necrosis factor receptor, interleukin-1 receptor (*IL1R*), *IL-1β*, *IL-6*, platelet-derived growth factor β chain, and *MCP-1*, was increased in apoE-KO mice compared with WT mice and decreased in DKO mice (Figure 4A and Supplemental Figure III). In addition, serum and aortic tissue MCP-1 protein levels were significantly decreased in DKO mice compared with apoE-KO mice (Figure 4B and 4C). Expression of mRNAs of intercellular adhesion molecule-1 (ICAM-1) and vascular cell adhesion molecule-1 (VCAM-1) was increased in atherosclerotic aortas of apoE-KO mice but significantly decreased in DKO mice (Figure 5A). Inducible nitric oxide synthase, expression of which is regulated by HH1R signaling in vascular SMCs,[26] was enhanced in apoE-KO mice and reduced in DKO mice (Supplemental Figure III).

Decreased Expression of MMPs in Atherosclerotic Aortas in DKO Mice

Expression of MMPs, which participate in the remodeling of atherosclerotic intima,[20,27,28] was increased in atherosclerotic plaques of apoE-KO mice, except for *MMP-9* after feeding with HcD for 12 weeks. In particular, *MMP-12* expression, which was hardly detected in the normal aortic tissue from WT mice, was markedly enhanced in apoE-KO mice. All the *MMP* mRNA expression investigated was significantly decreased in DKO mice (Figure 5A and Supplemental Figure III).

Decreased Expression and Nuclear Localization of NF-κB in Atherosclerotic Aortas in DKO Mice

One of the key regulators of inflammation, transcriptional factor NF-κB expression in the aortas, was evaluated by Western blotting and immunohistochemistry. In the atherosclerotic aortas of mice fed HcD for 12 weeks, expression was markedly increased in apoE-KO mice and decreased in DKO mice (Figure 5B). As shown by immunostaining, nuclear localization of NF-κB in the infiltrated macrophages, detected in apoE-KO mice, was decreased in DKO mice (Figure 5C).

Discussion

In the present study, we demonstrated that serum and aortic histamine contents and histamine receptor expression increased as hyperlipidemia-induced atherosclerosis developed in apoE-KO mice. In histamine-deficient DKO mice, atherosclerotic lesion was significantly attenuated despite the higher cholesterol levels. The expression of a range of proatherogenic cytokines, SRs, adhesion molecules, and MMPs in the aortas was reduced in DKO mice. Expression and activation of NF-κB, one of the key inflammatory regulators, was also decreased in DKO mice. Therefore, these results indicate that histamine promotes atherosclerosis independently of serum cholesterol levels but depending on gene regulation of inflammatory response.

Regulation of Atherosclerosis and Serum Lipid by Histamine

In both liver and atherosclerotic aortas, SR-BI expression were reduced in DKO compared with apoE-KO mice. HDL

cholesterol receptor SR-BI regulates reverse cholesterol transport from peripheral atherosclerotic lesions to the liver, and deletion of SR-BI in apoE-KO mice accelerates proatherogenic hypercholesterolemia and atherosclerosis.[23,29] Therefore, decreased expression of SR-BI is responsible in part for the increased cholesterol levels in DKO mice. In contrast, LDLR expression in the liver was moderately increased and that in the aortas was decreased in DKO mice. Because LDLR is expressed predominantly in the liver and LDLR-deficient mice show proatherogenic lipid profile because of reduced hepatic clearance of LDL and very-low-density lipoprotein,[30,31] it is probable that LDLR-mediated clearance of serum cholesterol would not, at least, be impaired in DKO mice.

In contrast, HDL cholesterol levels in DKO mice were higher than those in apoE-KO mice. The higher serum HDL cholesterol levels might partly participate in the reduction of atherosclerosis in DKO mice. Although the net effect of histamine deficiency on apoE-KO mice is attenuation of atherosclerosis with increased very-low-density lipoprotein, LDL, and HDL cholesterol, the exact mechanism(s) by which histamine regulates cholesterol metabolism is still unknown. Recently, however, we suggested that hepatic cholesterol accumulation is regulated by histamine signaling in the liver,[32] and therefore histamine actions mediated through histamine receptors expressed in tissues, including the artery and liver, probably regulate cholesterol metabolism.

On the other hand, SR-A, CD36, LOX-1, and SR-BI, which are the receptors for oxidized LDL and mainly expressed in atherosclerotic lesions to promote atherosclerosis,[22–25] were decreased in DKO mice. Partially supporting the present results, LOX-1 expression in monocytes is upregulated by histamine-mediated signal through HH2R.[17] Therefore, suppressed influx of modified LDL in aortas by histamine deficiency is implicated in reduced atherosclerosis progression in DKO mice in spite of increased serum cholesterol levels. In fact, atherosclerosis, which is enhanced in LDLR-KO or apoE-KO mice, is reduced by deficiency of LOX-1, SR-A, and CD36 expression.[33,34] Histamine is able to enhance cholesterol influx in peripheral tissues, resulting in the accumulation of cholesterol in lipid-laden cells in the aortas to accelerate atherosclerosis.

Regulation of Inflammatory Response by Histamine

Our study showed that proatherogenic cytokines and other molecules (such as IL-1β, IL-6, platelet-derived growth factor-BB, inducible nitric oxide synthase, and MCP-1) that regulate inflammatory response in the atherosclerotic lesions were markedly decreased along with attenuation of hyperlipidemia-induced atherosclerosis in DKO mice. Because influx of modified LDL into the atherosclerotic lesions also accelerates the inflammatory responses to the progress of atherosclerosis,[35,36] the decreased cholesterol influx contributes to the decreased inflammation to reduce atherosclerotic lesions in DKO mice.

Among those inflammatory factors, our previous studies showed histamine regulation of MCP-1 in relation to atherogenesis.[15,37,38] Histamine stimulates monocytes to express MCP-1 and its receptor CCR2, and it stimulates endothelial cells to upregulate ICAM-1 and VCAM-1 expression,[37] which are upregulated at atherosclerosis-prone sites in apoE-KO mice.[39] The expression of MCP-1 is also upregulated by granulocyte-macrophage colony-stimulating factor, which enhances the production of histamine via HDC expression of monocytes.[15,38] These data suggest that histamine modulates monocyte migration from peripheral blood via upregulation of MCP-1/CCR2 and adhesion molecules and that histamine is involved in an inflammatory network in the atherosclerotic lesion.[18] Actually, in the present study, the serum and aortic MCP-1 expression in DKO mice was significantly lower than that in apoE-KO mice. In addition, the aortic expression of endothelial and monocytic adhesion molecules, including ICAM-1 and VCAM-1, was induced in apoE-KO mice but significantly reduced in DKO mice. Because the increased expression of MCP-1 and adhesion molecules plays a central role in the progression and destabilization of established atherosclerosis in apoE-KO mice,[40] these data indicate that the antiatherogenic nature of DKO mice could, at least partially, be attributed to the downregulation of histamine-induced expression of MCP-1 and adhesion molecules.

Regulation of MMP Expression and Intimal Remodeling by Histamine

Transgenic expression or KO of MMP genes has been very often introduced in apoE-KO mice or another animal to investigate the relation between atherosclerosis and arterial matrix degradation.[41–43] Of special interest, the effects of MMP-9 and MMP-12 are well studied because of its elastolytic activity to destroy the arterial media for the progression of atherosclerosis. Indeed, we previously reported that MMP-12 plays an essential role in the invasion of macrophages into hypercholesterolemia-induced atherosclerotic foci in MMP-12 transgenic rabbits by disruption of elastic fibers.[20] The current data concerning MMPs indicate that histamine participates in tissue remodeling in hyperlipidemia-induced atherosclerosis via the expression of MMP-2, -3, -9, and -12. Although histamine is not able to directly induce these expression of these MMPs in cultured macrophages and SMCs (data not shown), the expression of MMPs is regulated by a complicated inflammation network including histamine in the atherosclerotic lesions.[18] It is of note that oxidized LDL–induced expression of MMP-2 and -9 in atherosclerotic lesions of LDLR-KO mice is mediated though activation of LOX-1,[44] because our previous study showed that histamine upregulates LOX-1 expression in monocytes.[17] The histamine-LOX-1-MMP axis may be present in atherosclerotic lesions to modulate extracellular matrix metabolism.

Regulation of NF-κB Signaling in Inflammatory Responses by Histamine

NF-κB signaling is critical for atherogenesis because it regulates vascular inflammatory responses, and activated NF-κB has demonstrated in atherosclerotic lesions.[45,46] Importantly, all the genes whose expression was decreased in DKO mice are targets of the transcriptional factor NF-κB in the atherosclerotic lesion.[45] Because the expression and

nuclear localization of NF-κB were decreased in DKO mice, these data indicate that histamine regulates NF-κB signaling in atherogenesis.

In conclusion, the present study indicates that the inflammatory response induced by histamine is an important regulator of atherosis induced by high serum cholesterol. Therefore, histamine could be a relevant therapeutic target in the treatment of atherosclerosis.

Acknowledgments

The authors thank Dr Masao Kimoto in the Faculty of Medicine, Saga University, for his critical suggestions and also to thank Hiroko Izakai, Hana Nishimura, Naoko Une, and Tomoko Shima for their expert technical assistance.

Sources of Funding

This work was supported in part by research grants from the Smoking Research Foundation (to A.T.) and by Grant-in-Aid 20590416 from the Japanese Ministry of Education, Science and Culture, Tokyo, Japan (to A.T. and Y.S.).

Disclosures

None.

References

1. Zelcer N, Tontonoz P. Liver X receptors as integrators of metabolic and inflammatory signaling. *J Clin Invest*. 2006;116:607–614.
2. Hansson GK. Inflammation, atherosclerosis, and coronary artery disease. *N Engl J Med*. 2005;352:1685–1695.
3. White MV. The role of histamine in allergic diseases. *J Allergy Clin Immunol*. 1990;86:599–605.
4. Brzozowski T, Konturek PC, Konturek SJ, Kwiecień S, Pajdo R, Drozdowicz D, Ptak A, Pawlik M, Hahn EG. Involvement of gastrin in gastric secretory and protective actions of *N*-α-methyl histamine. *J Physiol (Paris)*. 2001;95:89–98.
5. Forman MB, Oates JA, Robertson D, Robertson RM, Roberts LJ II, Virmani R. Increased adventitial mast cells in a patient with coronary spasm. *N Engl J Med*. 1985;313:1138–1141.
6. Laine P, Kaartinen M, Penttila A, Panula P, Paavonen T, Kovanen PT. Association between myocardial infarction and the mast cells in the adventitia of the infarct-related coronary artery. *Circulation*. 1999;99:361–369.
7. Steffel J, Akhmedov A, Greutert H, Lüscher TF, Tanner FC. Histamine induces tissue factor expression: implications for acute coronary syndromes. *Circulation*. 2005;112:341–349.
8. Knoflach M, Kiechl S, Mayr A, Willeit J, Poewe W, Wick G. Allergic Rhinitis, Asthma, and Atherosclerosis in the Bruneck and ARMY Studies. *Arch Intern Med*. 2005;165:2521–2526.
9. Iribarren C, Tolstykh IV, Eisner MD. Are patients with asthma at increased risk of coronary heart disease? *Int J Epidemiol*. 2004;33:743–748.
10. Clejan S, Japa S, Clemetson C, Hasabnis SS, David O, Talano JV. Blood histamine is associated with coronary artery disease, cardiac events and severity of inflammation and atherosclerosis. *J Cell Mol Med*. 2002;6:583–592.
11. Sasaguri Y, Wang KY, Tanimoto A, Tsutsui M, Ueno H, Murata Y, Kohno Y, Yamada S, Ohtsu H. Role of histamine produced by bone marrow-derived vascular cells in pathogenesis of atherosclerosis. *Cir Res*. 2005;96:974–981.
12. Takagishi T, Sasaguri Y, Nakano R, Arima N, Tanimoto A, Fukui H, Morimatsu M. Expression of the histamine H1 receptor gene in relation to atherosclerosis. *Am J Pathol*. 1995;146:981–988.
13. Nakashima Y, Fujii H, Sumiyoshi S, Wight TN, Sueishi K. Early human atherosclerosis: accumulation of lipid and proteoglycans in intimal thickenings followed by macrophage infiltration. *Arterioscler Thromb Vasc Biol*. 2007;27:1159–1165.
14. Higuchi S, Tanimoto A, Arima N, Xu H, Murata Y, Hamada T, Makishima K, Sasaguri Y. Effects of histamine and interleukin-4 synthesized in arterial intima on phagocytosis by monocytes/macrophages in relation to atherosclerosis. *FEBS Lett*. 2001;505:217–222.
15. Murata Y, Tanimoto A, Wang K-Y, Tsutsui M, Sasaguri Y, Corte FD, Matsushita H. Granulocyte macrophage–colony stimulating factor increases the expression of histamine and histamine receptors in monocytes/macrophages in relation to arteriosclerosis. *Arterioscler Thromb Vasc Biol*. 2005;25:430–435.
16. Wang KY, Arima N, Higuchi S, Shimajiri S, Tanimoto A, Murata Y, Hamada T, Sasaguri Y. Switch of histamine receptor expression from H2 to H1 during differentiation of monocytes into macrophages. *FEBS Lett*. 2000;473:345–348.
17. Tanimoto A, Murata Y, Nomaguchi M, Kimura S, Arima N, Xu H, Hamada T, Sasaguri Y. Histamine increases the expression of LOX-1 via H2 receptor in human monocytic THP-1 cells. *FEBS Lett*. 2001;508:345–349.
18. Tanimoto A, Sasaguri Y, Ohtsu H. Histamine network in atherosclerosis. *Trends Cardiovasc Med*. 2006;16:280–284.
19. Ohtsu H, Tanaka S, Terui T, Hori Y, Makabe-Kobayashi Y, Pejler G, Tchougounova E, Hellman L, Gertsenstein M, Hirasawa N, Sakurai E, Buzás E, Kovács P, Csaba G, Kittel Á, Okada M, Hara M, Mar L, Numayama-Tsuruta K, Ishigaki-Suzuki S, Ohuchi K, Ichikawa A, Falus A, Watanabe T, Nagy A. Mice lacking histidine decarboxylase exhibit abnormal mast cells. *FEBS Lett*. 2001;502:53–56.
20. Yamada S, Wang KY, Tanimoto A, Fan J, Shimajiri S, Kitajima S, Morimoto M, Tsutsui M, Watanabe T, Yasumoto K, Sasaguri Y. Matrix metalloproteinase 12 accelerates the initiation of atherosclerosis and stimulates the progression of fatty streaks to fibrous plaques in transgenic rabbits. *Am J Pathol*. 2008;172:1419–1429.
21. Usui S, Hara Y, Hosaki S, Okazaki M. A new on-line dual enzymatic method for simultaneous quantification of cholesterol and triglycerides in lipoproteins by HPLC. *J Lipid Res*. 2002;43:805–814.
22. Gough PJ, Greaves DR, Suzuki H, Hakkinen T, Hiltunen MO, Turunen M, Herttuala SY, Kodama T, Gordon S. Analysis of macrophage scavenger receptor (SR-A) expression in human aortic atherosclerotic lesions. *Arterioscler Thromb Vasc Biol*. 1999;19:461–471.
23. Acton S, Rigotti A, Landschulz KT, Xu S, Hobbs HH, Krieger M. Identification of scavenger receptor SR-B1 as a high density lipoprotein receptor. *Science*. 1996;271:518–520.
24. Park YM, Febbraio M, Silverstein RL. CD36 modulates migration of mouse and human macrophages in response to oxidized LDL and may contribute to macrophage trapping in the arterial intima. *J Clin Invest*. 2009;119:136–145.
25. Sawamura T, Kume N, Aoyama T, Moriwaki H, Hoshikawa H, Aiba Y, Tanaka T, Miwa S, Katsura Y, Kita T, Masaki T. An endothelial receptor for oxidized low-density lipoprotein. *Nature*. 1997;386:73–77.
26. Tanimoto A, Wang KY, Murata Y, Kimura S, Nomaguchi M, Nakata S, Tsutui M, Sasaguri Y. Histamine upregulates the expression of inducible nitric oxide synthase in human intimal smooth muscle cells via histamine H1 receptor and NF-κB signaling pathway. *Arterioscler Thromb Vasc Biol*. 2007;27:1556–1561.
27. Sasaguri Y, Yanagi H, Nagase H, Nakano R, Fukuda S, Morimatsu M. *Collagenase* production by immortalized human aortic endothelial cells infected with simian virus 40. *Virchows Arch B Cell Pathol Incl Mol Pathol*. 1991;60:91–97.
28. Sasaguri Y, Murahashi N, Sugama K, Kato S, Hiraoka K, Satoh T, Isomoto H, Morimatsu M. Development-related changes in matrix metalloproteinase expression in human aortic smooth muscle cells. *Lab Invest*. 1994;71:261–269.
29. Trigatti B, Rayburn H, Vinals M, Braun A, Miettinen H, Penman M, Hertz M, Schrenzel M, Amigo L, Rigotti A, Krieger M. Influence of the high density lipoprotein receptor SR-BI on reproductive and cardiovascular pathophysiology. *Proc Natl Acad Sci U S A*. 1999;96:9322–9327.
30. Ishibashi S, Brown MS, Goldstein JL, Gerard RD, Mammer RE, Herz J. Hypercholesterolemis in low density lipoprotine receptor knockout mice and its reversal by adenovirus-mediated gene delivery. *J Clin Invest*. 1993;92:883–893.
31. Osono Y, Woollett LA, Herz J, Dietschy JM. Role of the low density lipoprotein receptor in the flux of cholesterol through the plasma and across the tissue of the mouse. *J Clin Invest*. 1995;95:1124–1132.
32. Wang KY, Tanimoto A, Yamada S, Guo X, Ding Y, Watanabe T, Watanabe T, Kohno K, Hirano K, Tsukada H. Sasaguri Y. Histamine regulation in glucose and lipid metabolism via histamine receptors: model for nonalcoholic steatohepatitis in mice. *Am J Pathol*. 2010;177:713–723.
33. Mehta JL, Sanada N, Hu CP, Chen J, Dandapat A, Sugawara F, Satoh H, Inoue K, Kawase Y, Jishage K, Suzuki H, Yakeya M, Schnackenberg L, Berger R, Hermonat PL, Thomas M, Sawamura T. Deletion of LOX-1

reduces atherogenesis in LDLR knockout mice fed high cholesterol diet. *Circ Res.* 2007;100:1634–1642.
34. Manning-Tobin JJ, Moore KJ, Seimon TA, Bell SA, Sharuk M, Alvarez-Leite JI, de Winther MP, Tabas I, Freeman MW. Loss of SR-A and CD36 activity reduces atherosclerotic lesion complexity without abrogating foam cell formation in hyperlipidemic mice. *Arterioscler Thromb Vasc Biol.* 2009;29:19–26.
35. Khovidhunkit W, Kim MS, Memon RA, Shigenaga JK, Moser AH, Feingold KR, Grunfeld C. Effects of infection and inflammation on lipid and lipoprotein metabolism: mechanisms and consequences to the host. *J Lipid Res.* 2004;45:1169–1196.
36. Bensinger SJ, Tontonoz P. Integration of metabolism and inflammation by lipid-activated nuclear receptors. *Nature.* 2008;454:470–477.
37. Kimura S, Wang KY, Tanimoto A, Murata Y, Nakashima Y, Sasaguri Y. Acute inflammatory reactions caused by histamine via monocytes/macrophages chronically participate in the initiation and progression of atherosclerosis. *Pathol Int.* 2004;54:465–474.
38. Tanimoto A, Murata Y, Wand KY, Tsutsui M, Kohno K, Sasaguri Y. Monocyte chemoattractant protein-1 expression is enhanced by granulocyte-macrophage colony-stimulating factor via jak2-stat5 signaling and inhibited by atorvastatin in human monocytic U937 cells. *J Biol Chem.* 2008;283:4 643–4651.
39. Nakashima Y, Raines EW, Plump AS, Breslow JL, Ross R. Upregulation of VCAM-1 and ICAM-1 at atherosclerosis-prone sites on the endothelium in the apoE-deficient mouse. *Arterioscler Thromb Vasc Biol.* 1998;18:842–851.
40. Ni W, Egashira K, Kitamoto S, Kataoka C, Koyanagi M, Inoue S, Imaizumi K, Akiyama C, Nishida KI, Takeshita A. New anti-monocyte chemoattractant protein-1 gene therapy attenuates atherosclerosis in apolipoprotein E-knockout mice. *Circulation.* 2001;103:2096–2101.
41. Luttun A, Lutgens E, Manderveld A, Maris K, Collen D, Carmeliet P, Moons L. Loss of matrix metalloproteinase-9 or matrix metalloproteinase-12 protects apolipoprotein E-deficient mice against atherosclerotic media destruction but differentially affects plaque growth. *Circulation.* 2004;109:1408–1414.
42. Gough PJ, Gomez IG, Wille PT, Raines EW. Macrophage expression of active MMP-9 induces acute plaque disruption in apoE-deficient mice. *J Clin Invest.* 2006;116:59–69.
43. Kuzuya M, Nakamura K, Sasaki T, Cheng XW, Itohara S, Iguchi A. Effect of MMP-2-deficiency on atherosclerotic lesion formation in apoE-deficient mice. *Arterioscler Thromb Vasc Biol.* 2006;26:1120–1125.
44. Hu C, Dandapat A, Sun L, Chen J, Marwali MR, Romeo F, Sawamura T, Mehta JL. LOX-1 deletion decreases collagen accumulation in atherosclerotic plaque in low-density lipoprotein receptor knockout mice fed a high-cholesterol diet. *Cardiovasc Res.* 2008;79:287–293.
45. de Winther MPJ, Kanters E, Kraal G, Hofker MH. Nuclear factor κB signaling in atherogenesis. *Arterioscler Thromb Vasc Biol.* 2005;25:904–914.
46. Brand K, Page S, Rogler G, Bartsch A, Brandl R, Knuechel R, Page M, Kaltschmidt C, Bauerle PA, Neumeier D. Activated transcriptional factor nuclear factor-κB is present in the atherosclerotic lesion. *J Clin Invest.* 1996;97:1715–1722.

Supplemental Fig. I.

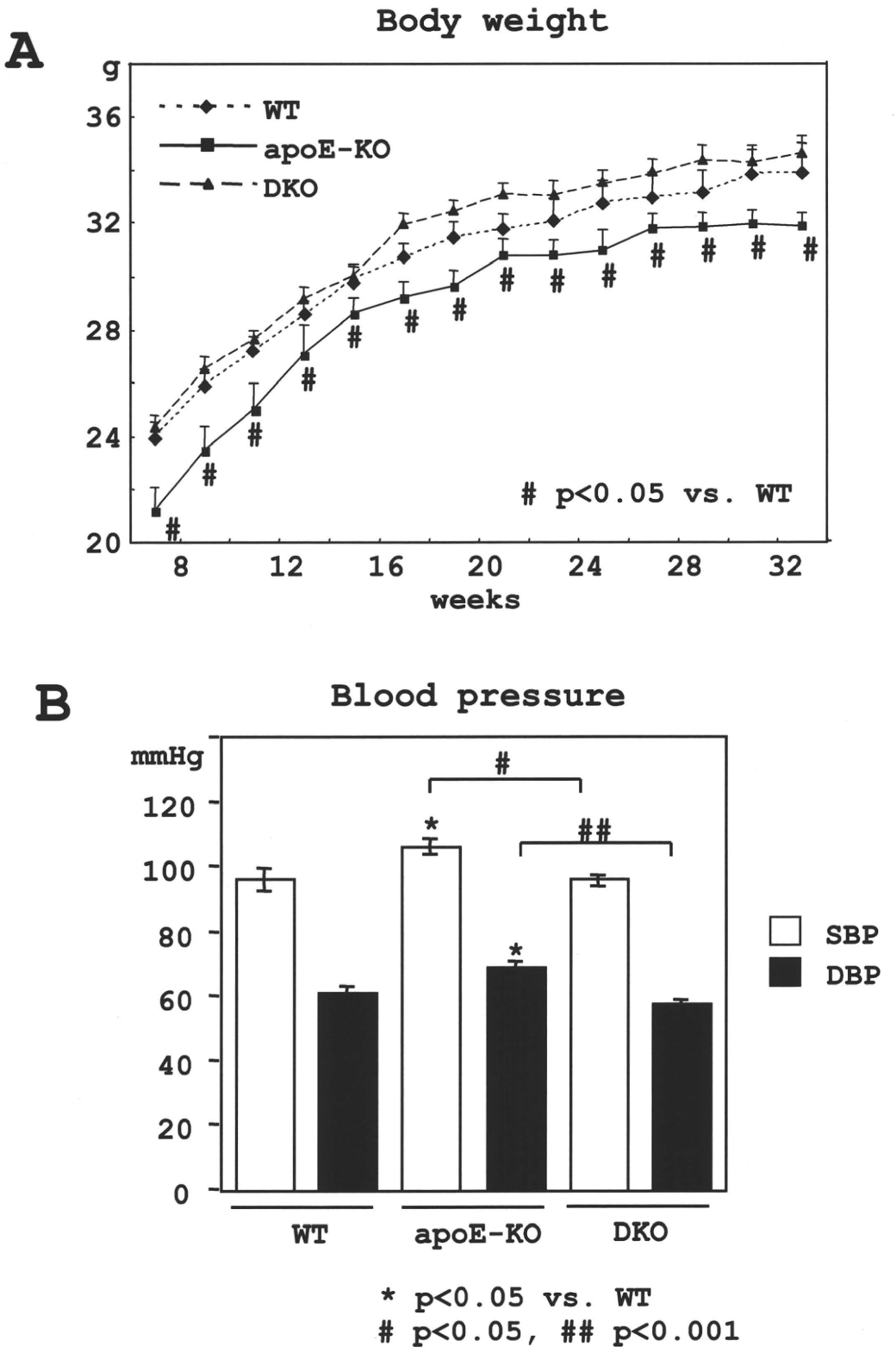

Supplemental Fig. II.

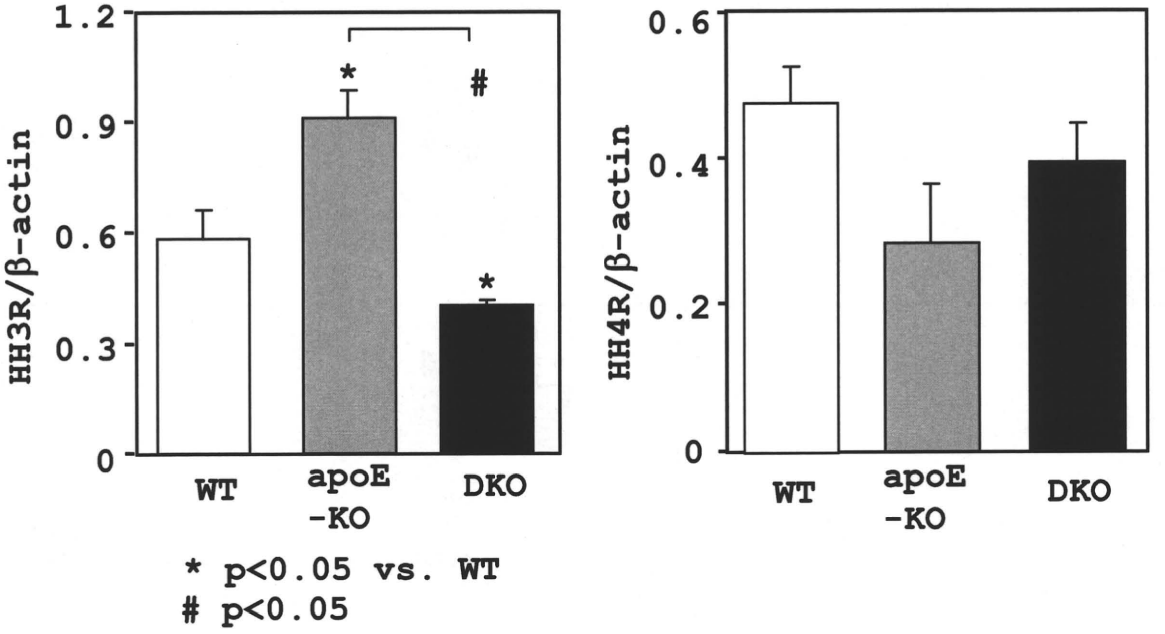

Supplemental Fig. III.

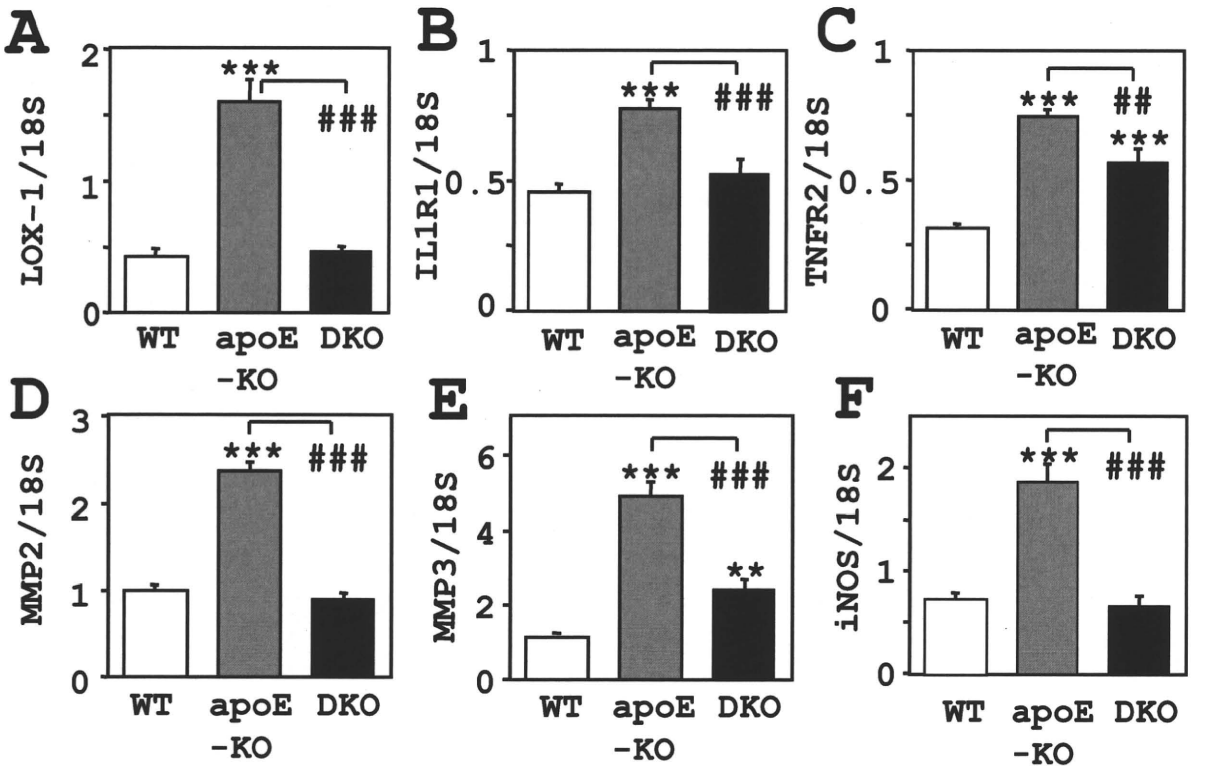

Table I.

Peripheral Blood Cell Count

	WBC(counts/μL)	NEU(%)	EOS(%)	BASO(%)	MONO(%)	LY(%)
WT	10992±1599	12.00±2.10	0.00±0.00	0.00±0.00	1.75±0.75	86.25±2.13
ApoE-KO	9125±1099	35.83±5.46*	0.16±0.16	0.00±0.00	2.66±0.98	61.33±5.80*
DKO	10296±1839	25.60±7.58	0.40±0.40	0.00±0.00	3.00±1.05	71.00±8.29

NEU, Neutrophile; EOS, eosinophile; BASO, Basophile; MONO, monocyte; LY, Lymphocyte
* $p<0.05$ vs. WT n=5

Femoral Bone Marrow Cell Counts

	WT	apoE-KO	DKO
Total cell counts($x10^7$/femur)	1.1±0.1	1.4±0.1	1.3±0.1
Erythroids(%)	32.1±6.5	25.3±4.8	28.9±6.3
Granuloids(%)	43.8±2.8	47.3±4.4*	44.2±3.6
Lymphocytes(%)	18.5±3.9	21.4±1.2	20.4±3.2
Monocytes(%)	5.2±1.5	4.9±0.8	5.9±2.5
Megakaryocytes(%)	0.1±0.1	0.2±0.2	0.2±0.2

* $p<0.05$ VS WT n=4

Table II.

CD3-positive T-Cell in aorta

counts/section	intima	media	adventitia
WT	0.00±0.00	0.00±0.00	0.69±0.23
apoE-KO	1.00±0.27*	0.00±0.00	1.75±0.39*
DKO	0.64±0.17*	0.00±0.00	1.57±0.27*

* $p<0.05$ vs. WT

Supplemental Text

Histamine Deficiency Decreases Atherosclerosis and Inflammatory Response in ApoE-KO Mice Independently on Serum Cholesterol Level

Ke-Yong Wang, [1] Akihide Tanimoto,[1, 2] Xin Guo, [1] Sohsuke Yamada,[1] Shohei Shimajiri,[1] Yoshitaka Murata,[3] Yan Ding,[1] Masato Tsutsui,[4] Seiya Kato,[5] TeruoWatanabe,[6] Hiroshi Ohtsu, [7] Ken-Ichi Hirano,[8] Kimitoshi Kohno, [9] and Yasuyuki Sasaguri[1*]

Departments of [1]Pathology and Cell Biology, and [9]Molecular Biology, School of Medicine, University of Occupational and Environmental Health, Kitakyushu 807-8555, Japan; [2]Department of Molecular and Cellular Pathology, Kagoshima University Graduate School of Medical and Dental Sciences, Kagoshima 890-8544, Japan; [3]Kyurin Omtest Laboratory Department, Kyurin Corp., Kitakyushu 806-0046, Japan; Departments of [4]Pharmacology, and [5]Pathology and Cell Biology, Graduate School and Faculty of Medicine, University of the Ryukyus, Okinawa 903-0215, Japan;[6] Laboratory of Pathology, Fukuoka Wajiro Hospital, Fukuoka 811-0213, Japan; [7]Department of Applied Quantum Medical Engineering, Tohoku University, Sendai 980-8579, Japan; [8]Department of Cardiovascular Medicine, Graduate School of Medicine, Osaka University, Osaka 565-0871, Japan.

*Corresponding author: Yasuyuki Sasaguri, MD, PhD, Department of Pathology and Cell Biology, School of Medicine, University of Occupational and Environmental Health, 1-1 Iseigaoka, Yahatanishi-ku, Kitakyushu 807-8555, Japan.

Tel: 81-93-691-7240, Fax: 81-93-603-8518, E-mail: yasu3219@med.uoeh-u.ac.jp

Materials and Methods

Measurement of blood pressure

The systolic and diastolic blood pressures were measured by tail-cuff method in 33-week-old mice fed NcD under conscious conditions (Model MK-2000, Muromachi Kikai Co., Ltd., Tokyo, Japan).

Hematopoietic cell counts in peripheral blood and bone marrow

The mice aged 33 wk fed NcD were used for the hematopoietic cell counts. Total white blood cell counts in the peripheral blood were calculated (counts/μL) and the leukocyte fractions (% to total count) were classified into neutrophiles, eosinophiles, basophiles, monocytes and lymphocytes. Total nucleated cells of the bone marrow (femur) were counted (counts/femur) and the fractions (% to total count) were classified into erythroids, granuloids, lymphocytes and megakaryocytes.

Mast cell counts in atherosclerotic lesions

The paraffin sections from the aortic lesions from 12-wk-HcD fed mice were stained by toluidine blue stain and mast cells were counted.

T lymphocyte counts in atherosclerotic lesions

The T lymphocytes in the atherosclerotic lesion from 12-wk-HcD fed mice were detected by immunohistochemistry using anti-CD3 antibody (rabbit polyclonal, x1; Dako) and positive cells were counted per section on a light microscope.

RT-PCR for HH3R and HH4R

The mRNA expression in the atherosclerotic lesions of 12-wk-HcD fed mice was

detected by RT-PCR using the primers listed below. For HH3R mRNA detection, the forward primer was 5'-AGCGCATGAAGATGGTATCC-3' and the reverse primer was 5'-AGCTTGGTGAAGGCTCTACG-3'. For HH4R mRNA detection, the forward primer was 5'-ATGGTAGGCAATGCTGTGG-3' and the reverse primer was 5'-TGTGTTCGTGCTGTTCTTCC-3'. As an internal control β-actin expression was monitored using the forward (FP) and reverse (RP) primers: FP 5'-TACATGGCTGGGGTGTTGAA-3' and RP 5'-AAGAGAGGCATCCTCACCC-3'.

Figure Legends

Supplemental Fig. I. Body weight and blood pressure in mice fed NcD.

A) Body weight curve of WT, apoE-KO and DKO mice up to 33-wk old. **B)** Blood pressure of the mice was measure at the age of 33 wk. Both systolic and diastolic blood pressures were lower in DKO mice than in apoE-KO mice.

Supplemental Fig. II. HH3R and HH4R expression in atherosclerotic lesions.

After feeding with HcD for 12 wk, HH3R mRNA but not HH4R expression was increased in apoE-KO mice, which was decreased in DKO mice.

Supplemental Fig. III. Expression of various inflammatory factors in atherosclerotic lesion.

After feeding with HcD for 12 wk, mRNA expression was monitored by real time RT-PCR. **A)** LOX-1 **B)** IL1R1 **C)** TNFR2 **D)** MMP2 **E)** MMP3 **F)** iNOS

All the expression was increased in apoE-KO mice than in WT mice and decreased in

DKO mice.

Journal of Cerebral Blood Flow & Metabolism (2011) 31, 305–314

www.jcbfm.com

Activation of the central histaminergic system is involved in hypoxia-induced stroke tolerance in adult mice

Yan-ying Fan[1,4], Wei-wei Hu[1,4], Hai-bin Dai[2,4], Jian-xiang Zhang[1], Lu-yi Zhang[1], Ping He[1], Yao Shen[1], Hiroshi Ohtsu[3], Er-qing Wei[1] and Zhong Chen[1]

[1]*Department of Pharmacology, Institute of Neuroscience, College of Pharmaceutical Sciences, Zhejiang University, Hangzhou, China;* [2]*Department of Pharmacy, Second Affiliated Hospital, School of Medicine, Zhejiang University, Hangzhou, China;* [3]*Department of Engineering, School of Medicine, Tohoku University, Aoba-ku, Sendai, Japan*

We hypothesized that activation of the central histaminergic system is required for neuroprotection induced by hypoxic preconditioning. Wild-type (WT) and histidine decarboxylase knockout (HDC-KO) mice were preconditioned by 3 hours of hypoxia (8% O_2) and, 48 hours later, subjected to 30 minutes of middle cerebral artery (MCA) occlusion, followed by 24 hours of reperfusion. Hypoxic preconditioning improved neurologic function and decreased infarct volume in WT or HDC-KO mice treated with histamine, but not in HDC-KO or WT mice treated with α-fluoromethylhistidine (α-FMH, an inhibitor of HDC). Laser-Doppler flowmetry analysis showed that hypoxic preconditioning ameliorated cerebral blood flow (CBF) in the periphery of the MCA territory during ischemia in WT mice but not in HDC-KO mice. Histamine decreased in the cortex of WT mice after 2, 3, and 4 hours of hypoxia, and HDC activity increased after 3 hours of hypoxia. Vascular endothelial growth factor (VEGF) mRNA and protein expressions showed a greater increase after hypoxia than those in HDC-KO or α-FMH-treated WT mice. In addition, the VEGF receptor-2 antagonist SU1498 prevented the protective effect of hypoxic preconditioning in infarct volume and reversed increased peripheral CBF in WT mice. Therefore, endogenous histamine is an essential mediator of hypoxic preconditioning. It may function by enhancing hypoxia-induced VEGF expression.
Journal of Cerebral Blood Flow & Metabolism (2011) **31**, 305–314; doi:10.1038/jcbfm.2010.94; published online 30 June 2010

Keywords: histamine; hypoxic preconditioning; vascular endothelial growth factor

Introduction

Cerebral ischemic tolerance is an adaptive process in which a brief subtoxic stress, such as hypoxic or ischemic preconditioning, induces endogenous neuroprotection against a subsequent severe ischemia. Alterations in the release of neurotransmitters and expression or activation of numerous proteins are involved in this process (Dirnagl *et al*, 2003), although the mechanisms are poorly understood. Knowledge of tolerance mechanisms may lead to identification of therapeutic targets to protect the brain either before surgery or in patients at high risk of stroke.

Histamine is recognized as an important neurotransmitter or neuromodulator in the central nervous system, which is synthesized from histidine by the specific enzyme, histidine decarboxylase (HDC) (Haas and Panula, 2003). Histaminergic neurons are located in the tuberomammillary nucleus of the posterior hypothalamus, and its fibers are widely distributed in the entire brain. Both *in vivo* and *in vitro* studies have indicated that histaminergic neurotransmission mediates neuroprotective activity through histamine H_1 or H_2 receptors, which are two postsynaptic receptors of histamine in the brain. Inhibition of histamine signaling by α-fluoromethyl-

Correspondence: Professor Z Chen, Department of Pharmacology, Institute of Neuroscience, College of Pharmaceutical Sciences, Zhejiang University, Hangzhou 310058, China.
E-mail: chenzhong@zju.edu.cn
[4]These authors contributed equally to this work.
This project was supported by the National Natural Science Foundation of China (30725047, 30572176, 30600757, 30801392), the National Basic Research of China 973 Program, (2009CB521906), and partly by the New Century Excellent Talents Program, Ministry of Education, China (NCET-06-0511), the Zhejiang Provincial Natural Science Foundation of China (Z207289), Youth foundation of the Innovative Scientific Research of Zhejiang University (2009QNA7007).
Received 31 January 2010; revised 11 May 2010; accepted 2 June 2010; published online 30 June 2010

histidine (α-FMH, a selective inhibitor of HDC) aggravates cerebral ischemic injury (Adachi, 2005). Through H_2 receptor activation, histamine prevents the severe damage to hippocampal CA1 pyramidal cells induced by transient forebrain ischemia (Adachi, 2005). *In vitro*, the H_1 receptor antagonist terfenadine enhances the excitotoxic response to NMDA (*N*-methyl-D-aspartic acid) in cerebellar neurons, and this is inhibited by histamine (Diaz-Trelles *et al*, 2000). Recently, we also reported that histamine protects against NMDA-induced necrosis in cultured cortical neurons through the H_2 receptor/cyclic AMP/PKA pathway (Dai *et al*, 2006). This evidence suggests that histamine has an important role in brain ischemia. In addition, an increase in histamine release occurs in synaptosomal preparations from rats with hypoxia (Waskiewicz *et al*, 1988), and in the rat cortex or striatum after focal cerebral ischemia (Adachi, 2005; Irisawa *et al*, 2008). However, the effect of histamine on hypoxia-induced stroke tolerance has not been examined.

Vascular endothelial growth factor (VEGF) has a key role in hypoxia-induced tolerance (Bernaudin *et al*, 2002; Laudenbach *et al*, 2007; Wick *et al*, 2002), moderates cerebral ischemic damage (Hayashi *et al*, 1998), and protects cultured neurons from hypoxia and glucose deprivation (Jin *et al*, 2000). Histamine is one of the main mediators of VEGF expression in various tissues and cells. In the granulation tissue, histamine enhances the content of the VEGF protein through the H_2 receptor (Ghosh *et al*, 2001), and HDC knockout (HDC-KO) mice show lower VEGF levels than do wild-type (WT) mice (Ghosh *et al*, 2002). Similarly, histamine increases VEGF production in cyclooxygenase-2-positive HT29 and Caco-2 cells, and this effect is prevented by H_2 antagonists (Cianchi *et al*, 2005). Thus, we hypothesized that endogenous histamine is involved in stroke tolerance induced by hypoxic preconditioning, and that this effect is associated with VEGF, although the relationship between them in the central nervous system remains unknown.

Materials and methods

Animals

Both WT and HDC-KO male mice (both are C57BL/6 strain) weighing 22 to 25 g were used, which were kindly provided by Professor Ohtsu (Liu *et al*, 2007). All experiments were conducted in accordance with the ethical guidelines of the Zhejiang University Animal Experimentation Committee and were in complete compliance with the National Institutes of Health Guide for the Care and Use of Laboratory Animals. Every effort was made to minimize any pain or discomfort, and the minimum number of animals was used.

Hypoxic Preconditioning and Drug Treatment *In Vivo*

Normobaric hypoxia (8% O_2) was achieved by replacing oxygen by nitrogen in an airtight chamber (5,500 mL). Hypoxic preconditioning was performed 48 hours before ischemia. In the α-FMH treatment group, α-FMH (25 mg/kg) was injected intraperitoneally 3 hours before hypoxia in WT mice. In the histamine treatment group of HDC-KO mice, histamine was administered intracerebroventricularly at a dose of 5 μg/2 μL per 6 h per animal for 3 injections in all, and the first injection was administered 30 minutes before hypoxia (i.e., 51.5, 45.5, and 39.5 hours before ischemia). The corresponding vehicle group and hypoxic preconditioning group of HDC-KO mice were injected with artificial cerebrospinal fluid three times by 2 μL/6 h per animal. SU1498 which is a VEGF receptor (VEGFR)2/Flk1 antagonist was administered intracerebroventricularly at a dose of 250 ng/2 μL per 12 h per animal for 3 injections in all WT mice, and the first injection was administered 30 minutes before hypoxia (i.e., 51.5, 39.5, and 27.5 hours before ischemia). The corresponding vehicle group and hypoxic preconditioning group of WT mice were injected with artificial cerebrospinal fluid containing 1% dimethyl sulfoxide three times by 2 μL/12 h per animal.

Transient Focal Cerebral Ischemia

Both WT and HDC-KO mice were anesthetized with an intraperitoneal injection of sodium pentobarbital (45 mg/kg). Cerebral blood flow (CBF) was determined in the territory of the middle cerebral artery (MCA) by laser Doppler flowmetry (Periflux System 5010; Perimed, Jarfalla, Sweden) as described previously (Inaba *et al*, 2009; Iwanami *et al*, 2007). A flexible fiberoptic probe was affixed to the skull over the cortex supplied by the proximal part (core; 2 mm caudal to the bregma and 6 mm lateral to midline) or the peripheral part (periphery; 2 mm caudal to the bregma and 3 mm lateral to midline) of the right MCA. The CBF in the core of the MCA territory was monitored in all animals subjected to MCA occlusion (MCAO), and in a part of animals, CBF in the periphery of the MCA territory was also monitored. Cerebral blood flow was expressed as a percentage of the value before MCAO. Animals with < 80% reduction in CBF in the core of the MCA territory were excluded from the study. The exclusion criteria used to eliminate mice from further consideration are shown in Supplementary Table 1.

Transient focal cerebral ischemia was induced by MCAO as described previously (Yu *et al*, 2005). Briefly, a 6-0 nylon monofilament suture, blunted at tip, and coated with 1% poly-L-lysine, was advanced 10 mm into the internal carotid to occlude the origin of MCA. Reperfusion was allowed after 30 minutes by monofilament removal. Body temperature was maintained at 37°C by a heat lamp (FHC, Bowdoinham, ME, USA) during surgery and for 2 hours after the start of reperfusion. Systolic blood pressure and heart rate were measured by a noninvasive tail cuff (ML 125 NIBP system, ADInstruments Pty Ltd., Castle Hill, NSW, Australia) connected to a PowerLab system (AD Instruments Pty Ltd., Castle Hill, NSW, Australia). Arterial pH, pO_2, and pCO_2 were monitored using an ABL700 series blood gas analyzer (Radiometer, Copenhagen, Denmark).

Neurologic deficit scores were evaluated as described previously (Longa *et al*, 1989) at 24 hours of reperfusion

as follows: 0, no deficit; 1, flexion of the contralateral forelimb on lifting of the whole animal by the tail; 2, circling to the contralateral side; 3, falling to contralateral side; and 4, no spontaneous motor activity.

Infarct volume was determined 24 hours after MCAO. The brains were quickly removed, sectioned coronally at 2-mm intervals, and stained by immersion in the vital dye 2,3,5-triphenyltetrazolium hydrochloride (TTC; 0.25%) at 37°C for 30 minutes. Extents of the normal and infarcted areas were analyzed using the ImageJ software (National Institutes of Health, Bethesda, MD, USA) and determined by the indirect method, which corrects for edema (contralateral hemisphere volume minus nonischemic ipsilateral hemisphere volume). The percentage of the corrected infarct volume was calculated by dividing the infarct volume by the total contralateral hemispheric volume, and this ratio was then multiplied by 100.

High-Performance Liquid Chromatography Determination of Histamine Concentration

Wild-type mice were killed immediately after 3 hours of hypoxia or normoxia, the brain was quickly removed, and the cerebral cortex was isolated and stored at −80°C until assay. The cerebral cortex was homogenized with 0.4 mol/L perchloric solution and centrifuged at 15,000 *g* for 20 minutes at 4°C, and the supernatant was collected. Analysis of histamine in each sample was performed by high-performance liquid chromatography (HPLC) as described previously (Jin *et al*, 2005). The HPLC was controlled, and data were acquired and analyzed using CoulArray software (ESA, Chelmsford, MA, USA). All equipments were obtained from ESA (Chelmsford, MA, USA).

Measurements of Histidine Decarboxylase Activity

Histidine decarboxylase activity was measured as described before (Shen *et al*, 2007). In short, the cerebral cortex was homogenized in 10-fold volume of ice-cold HDC buffer (0.1 mol/L potassium phosphate buffer, pH 6.8, 0.01 mmol/L pyridoxal-5′-phosphate, 0.2 mmol/L dithiothreitol, 1% polyethyleneglycol with average molecular weight of 300, 100 μg/mL phenylmethane sulfonylfluoride). The homogenates were centrifuged at 10,000 *g* for 15 minutes at 4°C, and 100 μL of the supernatant was transferred into a microcentrofilter tube (Ultracel YM-30, Millipore, Billerica, MA, USA). After centrifugation at 5,000 *g* for 40 minutes, 100 μL of the phosphate buffer was added to the pellet, which was gently suspended. This process was repeated twice to remove endogenous histamine. The enzymatic reaction was then started by adding 100 μL 1 mmol/L L-histidine at 37°C and the histamine produced during a 3-hour reaction was measured using HPLC.

Quantitative Real-Time PCR

Total RNA was isolated using a total RNA extraction kit, according to the manufacturer's instructions (Sangon, Shanghai, China). We then prepared cDNA using a Prime Script RT Reagent kit (Takara, Dalian, China) and performed quantitative real-time PCR with an ABI 7500 instrument (Applied Biosystems, Foster City, CA, USA) and a SYBR Green Real-time PCR Master Mix (Toyobo, Osaka, Japan). The following mouse primers were used: VEGF, 5′-GTAACGATGAAGCCCTGGAGT-3′ and 5′-TCAC ATCTGCTGTGCTGTAGGA-3′; erythropoietin, 5′-CCCACC CTGCTGCTTTTACT-3′ and 5′-ACAACCCATCGTGACATT TTCT-3′; HDC, 5′-ACCCCATCTACCTCCGACAT-3′ and 5′-ACCGAATCACAAACCACAGC-3′. Glyceraldehyde-3-phosphate dehydrogenase, 5′-GTCGGTGTGAACGGA;TTTGG-3′ and 5′-GCTCCTGGAAGATGGTGATGG-3′.

Immunoblotting

The cerebral cortex was homogenized, and total proteins were purified using cell and tissue protein extraction reagents according to the manufacturer's instructions (KC-415; KangChen, Shanghai, China). In all, 42 μg protein equivalent of each sample was electrophoresed on polyacrylamide gel, transferred onto nitrocellulose, and probed with monoclonal anti-VEGF antibodies (1:1,000; Abcam, Cambridge, UK), followed by IRDye 700-coupled anti-mice IgG (1:10,000; LI-COR Biosciences, Lincoln, NE, USA) secondary antibodies. Anti-glyceraldehyde-3-phosphate dehydrogenase antibody (1:5,000; KangChen, Shanghai, China) was used as the control. Blots were visualized using an Odyssey infrared imaging system (LI-COR Biosciences) and analyzed using Odyssey software. Relative optical densities were obtained by comparing measured values with the mean values from the WT control group.

Statistical Analysis

All data were collected and analyzed in a blind manner. Data are presented as mean ± s.e.m. One-way ANOVA (analysis of variance) with least significant difference (LSD) or Dunnett's T3 *post hoc* test (in which equal variances were not assumed) was applied for multiple comparisons, whereas Student's *t*-test was used for comparisons between two groups. Neurologic deficit scores were analyzed with the nonparametric Mann–Whitney *U*-test. $P<0.05$ was considered statistically significant.

Results

Hypoxic Preconditioning Induces Tolerance to Transient Focal Cerebral Ischemia in Wild-Type but Not in Histidine Decarboxylase Knockout Mice

During normobaric hypoxic preconditioning (8% O_2), animals displayed increased respiratory rate and reduced spontaneous movement. After preconditioning, they recovered within minutes. Two or three hours of hypoxia, performed 48 hours before transient MCAO, reduced infarct volume to 68.8% ($P<0.05$) or 50.5% ($P<0.05$) of the control group, respectively (Figure 1A). However, after a longer period of hypoxia (4 hours), the protection became weaker. The reduction in infarct volume in precon-